IL NUOVO CIMENTO **41 C** (2018) 185
DOI 10.1393/ncc/i2018-18185-5

Colloquia: IWM-EC 2018

Probing nucleon-nucleon correlations in heavy-ion transfer reactions

S. Szilner(1), L. Corradi(2), T. Mijatović(1), D. Montanari(3), F. Galtarossa(2), G. Pollarolo(4), G. Colucci(3), P. Čolović(1), E. Fioretto(2), A. Goasduff(3), D. Jelavić Malenica(1), G. Montagnoli(3), F. Scarlassara(3), N. Soić(1), A. M. Stefanini(2) and J. J. Valiente-Dobón(2)

(1) *Ruder Bošković Institute - Zagreb, Croatia*
(2) *INFN, Laboratori Nazionali di Legnaro - Legnaro, Italy*
(3) *Università di Padova and INFN, Sezione di Padova - Padova, Italy*
(4) *Università di Torino and INFN, Sezione di Torino - Torino, Italy*

received 3 December 2018

Summary. — Pair correlations have been investigated in heavy-ion collisions via studies of the transfers of different nucleon pairs. In particular, excitation functions of one- and two-neutron transfer channels have been measured for the closed shell ^{40}Ca + ^{96}Zr and superfluid ^{60}Ni + ^{116}Sn systems from the Coulomb barrier energy to energies far below. By using the unique performance of the magnetic spectrometer PRISMA, in terms of resolution and efficiency, measurements at very low bombarding energies have been performed. The experimental transfer probabilities have been compared with semiclassical microscopic calculations that incorporate nucleon-nucleon correlations, together with known structure information of entrance and exit channels nuclei and reaction dynamics. These calculations well reproduce, in the whole energy range, one- and two-neutron transfer channels in shape and magnitude.

1. – Introduction

Nucleon transfer reactions at energies close to the Coulomb barrier always played an important role for nuclear structure and reaction dynamics. Two-particle transfer reactions represents a very specific probe of pairing correlations in nuclear systems. The comparison between the measurement of two-particle transfer channels with the predictions using uncorrelated states should provide a direct measurement of the correlation of the populated states. Nucleon-nucleon correlations are particularly relevant in that they play an important role in stabilizing the system by increasing the binding energy of nuclei. Of particular interest is whether it is possible to reach a situation where multiple transfer of pairs is dominating the exchange of mass and charge between the interacting nuclei (Josephson effect).

In the collisions of heavy ions many degrees of freedom may participate and to extract the correlation effect from reaction observables requires, beside the use of the structure parameters, the correct modeling of the reaction dynamics. Unfortunately, in the majority of the available transfer data with heavy ions, the extraction of the enhancement factors due to the correlations was affected by ambiguities due to the complex reaction mechanism. In fact, almost all existing studies involve inclusive cross sections at energies higher than the Coulomb barrier, with the strong interplay between nuclear and Coulomb trajectories. On the contrary, at energies below the Coulomb barrier nuclei interact at very large distances, thus they are only slightly influenced by the nuclear potential and Q values are restricted to few MeV for the open transfer channels. These conditions diminish the complexity of calculations since only the overlap of the tails of the intrinsic wave functions that are involved in the transfer process have to be taken into account. Thus, we recently measured the transfer probabilities for one- and two-neutron transfer channels in heavy-ion collisions over the wide energy range with cross sections spanning several orders of magnitude. This energy regime is, on the other hand, characterized by low transfer cross sections. Only with the advent of large-solid-angle magnetic spectrometers the detection efficiency and resolution to identify the fragments in the heavy-ion collisions reached a sufficient level to make these experiments feasible [1, 2].

In this paper we will present the results of the measurements performed with the PRISMA spectrometer [2, 3]. First, selected results for measurements obtained above the Coulomb barrier will be presented in order to illustrate the main characteristics of the transfer mechanism. We will then concentrate on the measurements obtained far below the Coulomb barrier, where transfer cross sections obtained from excitation functions for the closed-shell ^{40}Ca + ^{96}Zr [4], and superfluid ^{60}Ni + ^{116}Sn [5] systems have been measured from the Coulomb barrier energy to energies corresponding to very large distances of closest approach. The experimental transfer probabilities will be compared with the microscopic calculations which incorporate nucleon-nucleon correlations. We would like to emphasize that, for the first time in a heavy-ion collision, we have been able to provide a consistent description of one- and two-neutron transfer reactions by incorporating, in the reaction mechanism, all known structure information of entrance and exit channel nuclei. This has to be considered a significant step forward in the understanding of two-neutron transfer processes.

2. – Transfer reactions at energy above and below the Coulomb barrier

Different techniques have been employed to identify nuclei produced in transfer reactions. Most of these techniques make use of magnetic spectrographs or spectrometers for a complete identification of nuclear charge, mass and energy of final reaction products. Magnetic spectrographs were mostly used in light-ion transfer reactions, where, by combining magnetic elements of different complexity to focus momenta, it was possible to distinguish the excited states (energy resolution of the order of a few tenths keV). With heavier ions more demanding conditions are required in order to keep a good resolution and to have at the same time a sufficient detection efficiency, given the large energy dynamic range of transfer products. For these ions, time-of-flight spectrometers have been designed with magnetic quadrupole elements which focus ions of different atomic charge states to a relatively small focal plane (see, *e.g.*, ref. [6]). The time-of-flight spectrometers provided a good A and Z resolution for medium mass ions, although with energy resolution of the order of a few MeV. These spectrographs or spectrometers have solid angles in the range 3–10 msr. Beyond these values, it becomes unfeasible to use complex

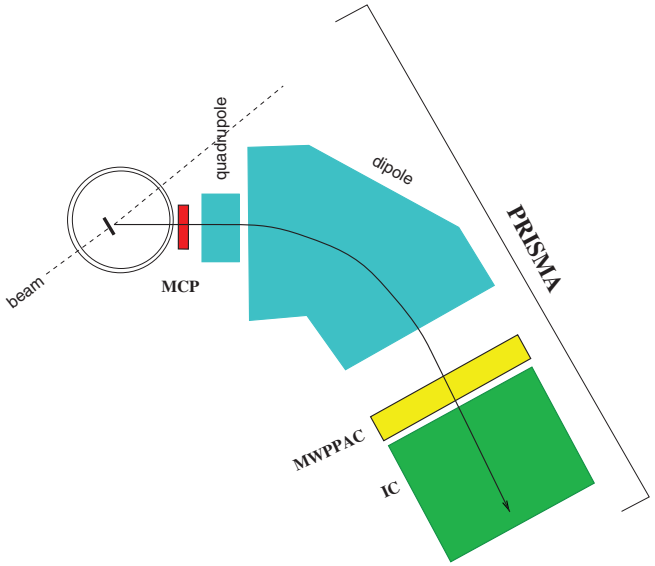

Fig. 1. – Layout of the PRISMA spectrometer, MCP: micro-channel plate detector; MWPPAC: parallel-plate detector of multiwire type; IC: ionization chamber.

magnetic elements to correct for the ion optical aberrations. The solution for the large-solid-angle spectrometers (∼100 msr) was to simplify the magnetic element configuration and to apply the concept of trajectory reconstruction [3, 7-9], by using a detector system which, besides nuclear charge, energy and timing, provides the necessary position information along the ion path. With these new generation spectrometers, mass and nuclear charge identification has been successfully demonstrated for ions up to A∼100–130, but energy resolution is presently limited to few hundreds of keV. This was compensated by coupling the spectrometers with the high purity germanium gamma array [10-12].

To illustrate the main working principle of the large solid angle spectrometers, we here briefly list the main characteristics of the PRISMA spectrometer and its detector system (see fig. 1). A position-sensitive micro-channel plate detector [13] is placed at the entrance of the spectrometer, providing a start signal for time-of-flight measurements and bi-dimensional position signals. Ions pass through the optical elements of the spectrometer (a quadrupole and a dipole) and enter a focal plane detector [14] which is made of a parallel plate detector of multiwire type, providing timing and bi-dimensional position signals with resolutions similar to the entrance detector. Located at the end of the focal plane is an array of transverse field multiparametric ionization chambers (IC), providing nuclear charge via energy loss (ΔE) and total energy (E) measurements. The detector system gives all the necessary information for the complete ion identification, which is performed via an event-by-event reconstruction of the trajectory inside the magnetic elements [2, 15, 16].

To illustrate the main characteristic of the multinucleon transfer reaction mechanism, we plot in fig. 2 the experimental transfer cross sections of ^{58}Ni + ^{208}Pb [17], ^{40}Ca + ^{208}Pb [18], and ^{40}Ar + ^{208}Pb [19] measured at comparable energies above the Coulomb barrier. Such comparison between different systems is significant for understanding the importance of the different degrees of freedom that influence the evolution of the reaction.

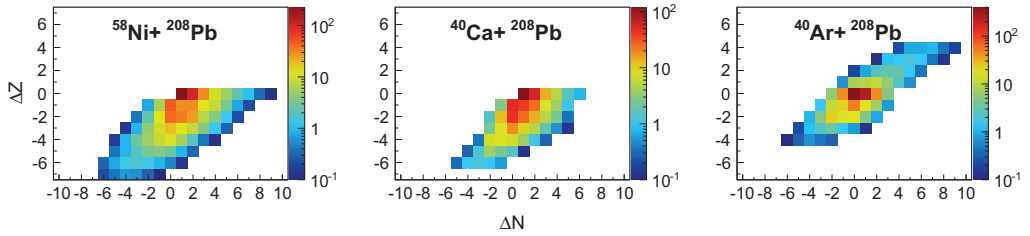

Fig. 2. – Angle and energy integrated total cross section for ^{40}Ar, ^{40}Ca, and ^{58}Ni projectiles on the ^{208}Pb target, at energies $E_{\rm lab}$ = 6.4, 6.2, and 6 MeV/A, respectively. The cross section values of the elastic(+inelastic) channel, with ΔN and $\Delta Z = 0$, have been scaled down by a factor 100 to better display the behavior of the transfer channels.

While with the "neutron-poor" ^{40}Ca and ^{58}Ni beams the reaction mechanism strongly favors the proton stripping and neutron pickup channels, it is evident how the transfer flux changes with the use of the neutron-richer ^{40}Ar beam. In particular, one sees how proton pickup channels open up. Close to the entrance channel mass partition the relative strength of the different channels is compatible with the quasielastic character of the reaction which is mainly governed by optimum Q values and nuclear structure properties. One also can notice how for the many-proton transfer channels, the mass distributions shift toward lower values, indicating the presence of the secondary processes. The large energy losses observed in these channels may lead to neutron evaporation, which strongly affects the lower-mass region of all populated isotopes.

The experimental cross sections have been compared with different semiclassical models [17-20]. These models particularly well describes the one-nucleon transfer channels, while the deviations between experimental data and calculations are more marked for channels involving the transfer of pairs of nucleons, in particular in the proton sector. This fact has been discussed in our previous publications [17, 18] where the inclusion of the pair-transfer modes (both for neutrons and protons) was crucial in the description of the calculated cross sections. However, it was pointed out that the contribution from deep-inelastic processes as we move away from the entrance channel mass partition, may obscure the quantitative conclusion of the effect of the pair-transfer.

To diminish the complexity of the reaction mechanism we performed the series of measurements below the Coulomb barrier. At these energies measurements of heavy-ion transfer reactions have significant technical difficulties. This is the main reason why available data are extremely scarce or almost non-existing. In direct kinematics the transfer probability at large distances corresponds to fragments that are scattered at forward angles. In this angular range the overwhelming yield of elastically scattered particles often prevents a good identification for isotopes close to the projectile. To partly overcome these problems, we made use of inverse kinematics, *i.e.* we detected the lighter target-like particles with the PRISMA magnetic spectrometer at forward angles. In this way, a larger efficiency (kinematic focusing) and a better resolution (high kinetic energy) have been obtained.

In the measured reactions, ^{96}Zr + ^{40}Ca and ^{116}Sn + ^{60}Ni, (lighter) target recoils have been detected with PRISMA, and the excitation functions at several bombarding energies have been obtained from the Coulomb barrier to 20–25% below, reaching ∼15.5 fm of distance of closest approach. The identification of fragments has been done on an event-by-event basis by using, for the atomic number, the range of the ions as a function of the

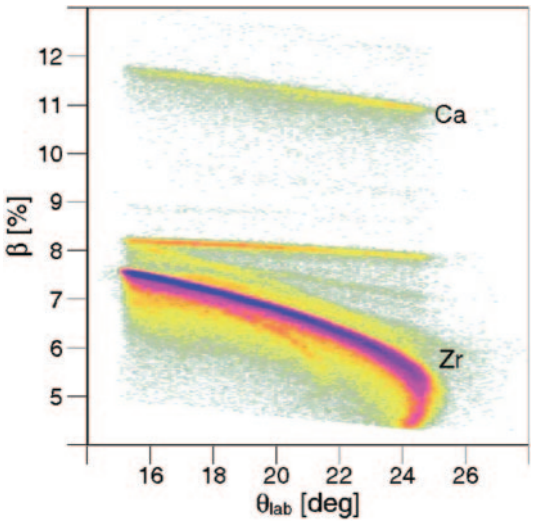

Fig. 3. – Velocity ($\beta = v/c$) *vs.* in-plane scattering angle ($\theta_{\rm lab}$) for the reaction ^{96}Zr + ^{40}Ca at $E_{\rm lab} = 330$ MeV. The magnetic fields of the spectrometer were set to bring the Ca ions with maximum yield near the center of the focal plane area. The events at large β correspond to Ca-like recoils, and those at lower β to Zr-like ions scattered from Ca, as well as from other elements in the target (from ref. [4]).

total energy released in the ionization chamber and, for the mass, by reconstructing the trajectories of the ions inside the magnetic elements of PRISMA [2, 3, 15, 16, 19].

A fingerprint of the inverse kinematic is the behavior of the velocity as a function of in-plane scattering angle. Such matrix, for the ^{96}Zr + ^{40}Ca reaction, is displayed in fig. 3. One sees the events corresponding to Ca-like recoils as well as those corresponding to Zr-like ions. The ridges of these Zr-like ions are due to scattering on Ca (main ridge presenting a bending around the kinematic limiting angle), on lighter elements (with smaller limiting angles), and on other heavier elements. The almost horizontal ridge, with high yield and with a $\beta \sim 0.08$, is due to Zr scattering in direct kinematics.

To illustrate the obtained mass resolution and the clear separation of different isotopes we show, as an example, the mass spectra at selected energies for the ^{96}Zr + ^{40}Ca reaction in fig. 4. At the higher energies, close to and above the Coulomb barrier, more than four neutrons have been transferred, while at the sub-barrier energies only one or at most two neutron transfers survive. Very similar mass distributions have been also observed for the ^{116}Sn + ^{60}Ni reaction. To see the behavior of the energy distributions we plot in fig. 5 the total kinetic energy loss (TKEL) distributions for the elastic(+inelastic), one- and two-neutron transfer channels obtained in the "direct" ^{40}Ca + ^{96}Zr [2] and inverse kinematic ^{96}Zr + ^{40}Ca [4] measurements at the indicated center of mass energies. These TKEL were constructed assuming a binary reaction and imposing the conservation of momentum. One notices how the width of the TKEL distributions become narrower with the decrease of the energy. At the lowest energy it is compatible with the expected energy resolution due to the intrinsic detector resolution, the effect of the trajectory reconstruction procedure, beam position and angle indetermination on target and target straggling effects.

In general, with heavy ions, due to the illustrated limitation in the energy resolution with particle detectors, it is mandatory to combine such detectors with the gamma

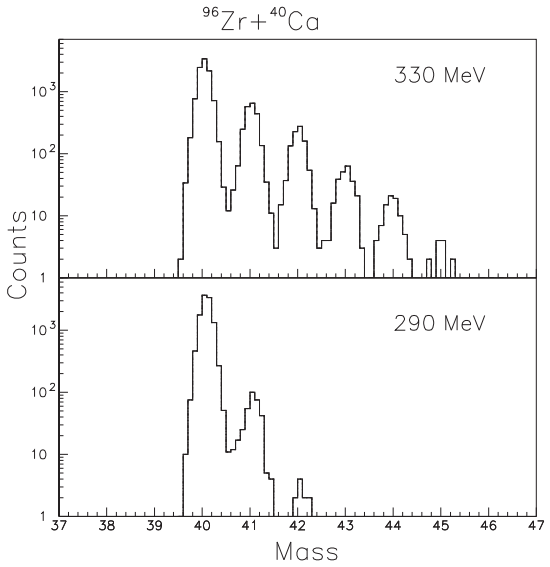

Fig. 4. – Mass distributions for pure neutron transfer channels obtained in the reaction ^{96}Zr + ^{40}Ca at the indicated bombarding energies of the ^{96}Zr beam, and with the Ca-like recoils detected in PRISMA.

detection in order to distinguish the single excited states. Thus, we performed an additional particle-gamma coincidence experiment for the ^{60}Ni + ^{116}Sn system by using the PRISMA spectrometer coupled to the Advanced Gamma Tracking Array (AGATA) demonstrator [12, 21, 22]. The demonstrator configuration included four triple cluster modules providing a simulated full-absorption efficiency of 2.64% for 1.3 MeV γ-rays. We used a ^{60}Ni beam at 245 MeV on the ^{116}Sn target, and detected the Ni-like fragments in PRISMA placed at 70°, the laboratory angle which corresponds to large distances of closest approach. This particle-γ coincidence measurement allowed to estimate the fraction of the total cross section going into excited states. In the inelastic channel the dominant transitions were from the 2^+ states of the binary partners. In the one-neutron transfer channel, a strong population of the low lying states of the single particle character has been observed, in particular the population of the $1/2^-$ state in ^{61}Ni and of the $5/2^+$ state in ^{115}Sn. For the two-neutron transfer channel we observed only a few events compatible with the transition from the 2^+ state to the 0^+ ground state of ^{62}Ni. For this two-neutron transfer channel, from the experimental intensities of the γ lines, we concluded that the strength going to excited states is less than 24% of the total transfer strength of this channel. This finding indicates a dominance of the ground-to-ground state transition in this two-neutron transfer channel.

3. – Nucleon-nucleon correlations

In order to have an overall description of the experimental data it is convenient to extract the transfer probability $P_{\rm tr}$, defined as the ratio of the transfer cross section to the corresponding Rutherford cross section, and to plot these probabilities as a function of the distance of closest approach D for a Coulomb trajectory. The extraction of the transfer probability $P_{\rm tr}$ is rather alluring because the angular distributions obtained at different

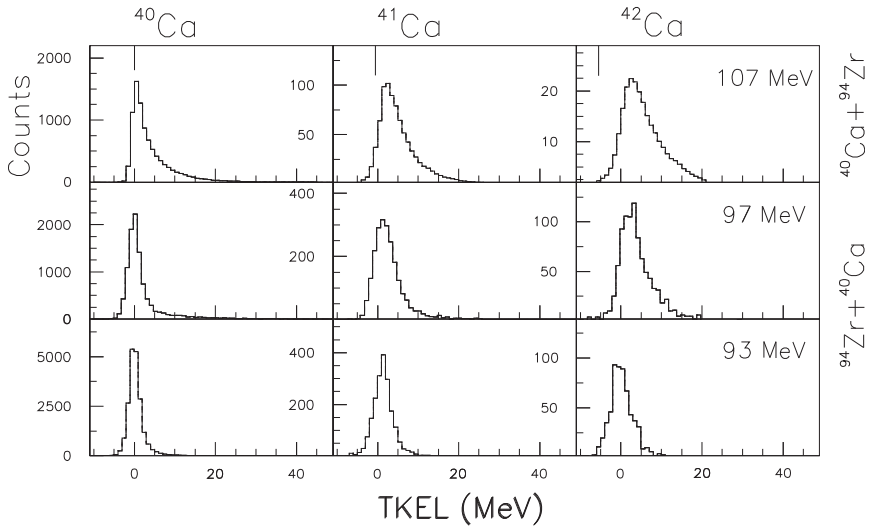

Fig. 5. – Experimental TKEL distributions for the elastic(+inelastic), one- and two-neutron transfer channels obtained in the "direct" ^{40}Ca + ^{96}Zr [2] and inverse kinematic ^{96}Zr + ^{40}Ca [4] measurements at the indicated center-of-mass energies. These energies correspond to about 10% above, at, and 10% below the Coulomb barrier. The vertical lines represent the ground-state Q values: $Q^{1n}_{\rm gs} = +0.5\,$MeV and $Q^{2n}_{\rm gs} = +5.5\,$MeV.

bombarding energies will be all superimposed, if the Q-value window does not change significantly. Further, the transfer probability at large distances D may be obtained by measuring an excitation function at fixed center of mass angle or by measuring angular distributions at fixed energy. The transfer probabilities for the ^{116}Sn + ^{60}Ni measurement are presented (full symbols), together with the calculations, in fig. 6 for the $(1n)$ and $(2n)$ neutron transfer channels.

The transfer probabilities have been analyzed by employing a microscopic theory, which, for the first time in a heavy-ion collision, provided a consistent description of one- and two-neutron transfer channels, in shape and magnitude. In more details, to compute the inelastic and one-neutron transfer channels the calculations have been performed by employing the same optical potential. Taking into account the collectivity of the low-lying states of the target and the projectile and the strong Coulomb field, a coupled-channels calculation have been performed for the inelastic channel by including the states which have been strongly populated in the particle-γ measurement in the vibrational approximation and with the tabulated values for the deformation parameters. For the one-neutron transfer channel the calculations have been performed in the DWBA approximation. These calculations provide, in good approximation, the direct population of states which can be compared with the experimental intensities obtained in the particle-γ measurement. Such comparisons provide a direct check on the one-particle form factors that have been used in the successive approximation for the two-neutron transfer. The transfer probability for the inclusive $(1n)$ channel (full black line in fig. 6) has been calculated by summing over all possible transitions that can be constructed from the single particle states in projectile and target (see refs. [4, 5]), and by weighting each transition with the corresponding spectroscopic factor. For both systems, the calculations agree well with the experimental transfer probabilities.

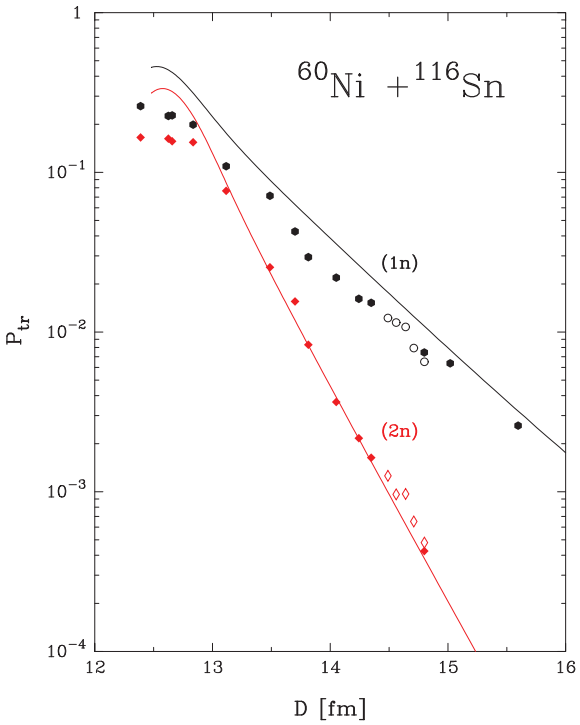

Fig. 6. – Experimental (points) and microscopically calculated (lines) transfer probabilities P_{tr} as a function of the distance of closest approach D for one- (^{61}Ni) and two-neutron (^{62}Ni) transfers in the ^{60}Ni + ^{116}Sn system (from ref. [23]).

To calculate the $(2n)$ channel one has to solve the well-known system of semiclassical coupled equations up to the second-order Born approximation. The amplitude consists of three terms, the simultaneous transfer of the pair of nucleons, the nonorthogonality term, and the term which represents the successive process via an intermediate channel. For the calculation of the $(2n)$ channel the ground-to-ground state transition has been included following the formalism of ref. [24]. In this formalism one can employ the same single-particle form factors used for the $(1n)$ channel. The ground states have been described in the BCS approximation with a standard state-independent pairing force.

For the $(2n)$ channel of the ^{60}Ni + ^{116}Sn system (see fig. 6) the experimental points are very well described by the calculation. This fact indicates that the two-neutron transfer channel in this system is populating essentially only the ground state, in agreement with the experimental total kinetic-energy loss distributions where the transfer strength was clearly concentrated around the ground state. Even more, the particle-γ measurement provided the upper limit for the possible excited state population in the $(2n)$ channel.

It is very important to stress that the shown results are not coming from best-fit procedure, but that they employed a microscopic theory that incorporates nucleon-nucleon correlations.

4. – Summary and outlook

The advent of the large-solid-angle magnetic spectrometers, coupled to large γ arrays, ensured significant advances in the field of multinucleon transfer reactions at energies

close to the Coulomb barrier. We presented recent results of reactions measured with the PRISMA spectrometer. The correlations were discussed via transfer probabilities for one- and two-neutron transfer channels in the ^{40}Ca + ^{96}Zr and ^{60}Ni + ^{116}Sn systems. These probabilities have been compared with microscopic theory that incorporates nucleon-nucleon correlations. The employed theory very well reproduces the experimental data in the whole energy range, in particular, the transfer probability for two neutrons in the Q-value matched ^{60}Ni + ^{116}Sn system is very well reproduced, in magnitude and slope, by considering solely the ground-to-ground state transition. It is very important to continue these studies, and to compare the experimental observables with microscopic calculations where nucleon-nucleon correlations are treated together with the relevant structure and dynamics information.

As a follow-up of these results, it will be important to study whether and to what extent the effect of neutron-neutron correlations, in the evolution of the reaction, is modified in the presence of high Coulomb fields. Thus, we very recently measured the probability for neutron transfer channels in the reaction ^{206}Pb + ^{118}Sn in a wide range of distance of closest approach. The measurement was performed in inverse kinematics by using the newly developed ^{206}Pb beam at superconducting PIAVE-ALPI accelerators. This is the heaviest (asymmetric) semi-magic system with closed proton and open neutron shells, very well Q-value matched for neutron transfers. In very heavy-ion collisions, the population of final states with high excitation energies and large angular momenta may significantly change the transfer strength of the ground-to-ground state transitions.

The issue connected with the pair correlations is presently at the focus of a renewal of interest [25-35], in particular in ongoing research with radioactive beams, where the pairing interaction may be significantly modified in nuclei with extended neutron distributions [36].

* * *

The authors acknowledge financial support from the European Regional Development Fund for the Center of Excellence for Advanced Materials and Sensing Devices (Grant No. KK.01.1.1.01.0001). This work was also partly supported by the Croatian Science Foundation under Project No. 7194.

REFERENCES

[1] Corradi L., Pollarolo G. and Szilner S., *J. Phys. G*, **36** (2009) 113101.
[2] Szilner S. *et al.*, *Phys. Rev. C*, **74** (2007) 024604.
[3] Corradi L. *et al.*, *Nucl. Instrum. Methods Phys. Res. B*, **317** (2013) 743.
[4] Corradi L. *et al.*, *Phys. Rev. C*, **84** (2011) 034603.
[5] Montanari D. *et al.*, *Phys. Rev. Lett.*, **113** (2014) 052501.
[6] Montagnoli G. *et al.*, *Nucl. Instrum. Methods Phys. Res. A*, **454** (2000) 306.
[7] Fioretto E. *et al.*, *Nucl. Instrum. Methods Phys. Res. B*, **899** (2018) 73.
[8] Pullanhiotan S. *et al.*, *Nucl. Instrum. Methods Phys. Res. A*, **593** (2008) 343.
[9] Cappuzzello F. *et al.*, *Eur. Phys. J. A*, **52** (2016) 167.
[10] Gadea A. *et al.*, *Eur. Phys. J. A*, **20** (2004) 193.
[11] Simpson J. *et al.*, *Acta Physica Hungarica N.S.*, **11** (2000) 159.
[12] Gadea A. *et al.*, *Nucl. Instrum. Methods Phys. Res. A*, **654** (2011) 88.
[13] Montagnoli G. *et al.*, *Nucl. Instrum. Methods Phys. Res. A*, **547** (2005) 455.
[14] Beghini S. *et al.*, *Nucl. Instrum. Methods Phys. Res. A*, **551** (2005) 364.
[15] Montanari D. *et al.*, *Eur. Phys. J. A*, **47** (2011) 4.
[16] Mijatovic T. *et al.*, *Eur. Phys. J. A*, **52** (2016) 113.

[17] Corradi L. *et al.*, *Phys. Rev. C*, **66** (2002) 024606.
[18] Szilner S. *et al.*, *Phys. Rev. C*, **71** (2005) 044610.
[19] Mijatovic T. *et al.*, *Phys. Rev. C*, **94** (2016) 064616.
[20] Galtarossa F. *et al.*, *Phys. Rev. C*, **97** (2018) 054606.
[21] Farnea E. *et al.*, *Nucl. Instrum. Methods Phys. Res. A*, **621** (2010) 331.
[22] Akkoyun S. *et al.*, *Nucl. Instrum. Methods Phys. Res. A*, **668** (2012) 26.
[23] Montanari D. *et al.*, *Phys. Rev. C*, **93** (2016) 054623.
[24] Sorensen J. H. and Winther A., *Nucl. Phys. A*, **550** (1992) 306.
[25] Simenel C., *Phys. Rev. Lett.*, **105** (2010) 192701.
[26] Evers M. *et al.*, *Phys. Rev. C*, **84** (2011) 054614.
[27] Potel G. *et al.*, *Phys. Rev. Lett.*, **107** (2011) 092501.
[28] Broglia R. A. *et al.*, *Phys. Scr.*, **91** (2016) 063012.
[29] Lemasson A. *et al.*, *Phys. Lett. B*, **697** (2011) 454.
[30] Scamps G. and Lacroix D., *Phys. Rev. C*, **87** (2013) 014605.
[31] Scamps G. and Hagino K., *Phys. Rev. C*, **92** (2015) 064602.
[32] Scamps G. *et al.*, *Phys. Rev. C*, **94** (2016) 064606.
[33] Sekizawa K. and Yabana K., *Phys. Rev. C*, **88** (2013) 014614.
[34] Magierski P., Sekizawa K. and Wlazlowski G., *Phys. Rev. Lett.*, **119** (2017) 042501.
[35] Dobaczewski J., Nazarewicz W., Werner T. R., Berger J. F. and Decharge J., *Phys. Rev. C*, **53** (1996) 2809.
[36] Dobaczewski J. *et al.*, *Phys. Rev. Lett.*, **72** (1994) 981.